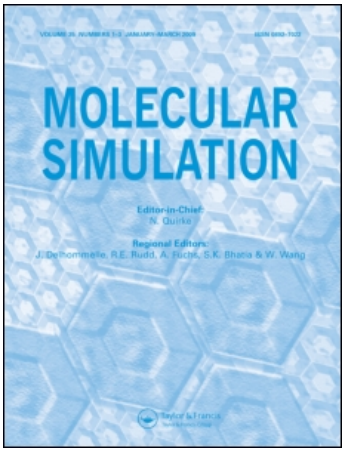

Molecular Simulation
Publication details, including instructions for authors and subscription information:
http://www.informaworld.com/smpp/title~content=t713644482

Molecular dynamics simulations of carbon nanotube oscillators deformed by encapsulated copper nanowires

Jeong Won Kang[a]; Young Gyu Choi[a]; Jun Ha Lee[b]; Oh Kuen Kwon[c]; Ho Jung Hwang[d]
[a] Department of Computer Engineering, Chungju National University, Chungju, South Korea [b] Department of Computer System Engineering, Sangmyung University, Chonan, South Korea [c] Department of Electronic Engineering, Semyung University, Jecheon, South Korea [d] Electrical and Electronic Engineering School, Chung-Ang University, Seoul, South Korea

To cite this Article Kang, Jeong Won , Choi, Young Gyu , Lee, Jun Ha , Kwon, Oh Kuen and Hwang, Ho Jung(2008) 'Molecular dynamics simulations of carbon nanotube oscillators deformed by encapsulated copper nanowires', Molecular Simulation, 34: 9, 829 — 835
To link to this Article: DOI: 10.1080/08927020802301953
URL: http://dx.doi.org/10.1080/08927020802301953

Molecular Simulation
Vol. 34, No. 9, August 2008, 829–835

Taylor & Francis
Taylor & Francis Group

Molecular dynamics simulations of carbon nanotube oscillators deformed by encapsulated copper nanowires

Jeong Won Kang[a], Young Gyu Choi[a], Jun Ha Lee[b], Oh Kuen Kwon[c] and Ho Jung Hwang[d]*

[a]*Department of Computer Engineering, Chungju National University, Chungju, South Korea;* [b]*Department of Computer System Engineering, Sangmyung University, Chonan, South Korea;* [c]*Department of Electronic Engineering, Semyung University, Jecheon, South Korea;* [d]*Electrical and Electronic Engineering School, Chung-Ang University, Seoul, South Korea*

(*Received 23 June 2008; final version received 25 June 2008*)

Pure carbon nanotube (CNT) oscillators are compared to the corresponding CNT oscillators encapsulating copper nanowires (Cu@CNTs) by molecular dynamics simulations. The classical oscillation theory provides a fairly good estimate of the mass dependence of the operating frequency when the CNT surface is not deformed by the Cu nanowire. The structural deformations of the CNT induced by the encapsulated copper nanowire have a greater effect on the oscillation frequency than the mass of the copper nanowire. The excess forces of the Cu@CNT oscillator are slightly higher than those of the CNT oscillator and the excess van der Waals forces induced by the inter-wall interactions are 17 times higher than the excess forces induced by the Cu nanowire–CNT interactions.

Keywords: nanotube oscillators; gigahertz oscillators; molecular dynamics

1. Introduction

After Cumings and Zettl [1] reported an ideal low-friction and low-wear bearing carved out of a multi-walled carbon nanotube (CNT) with a diameter of a few tens of nanometers, gigahertz CNT-based oscillators were proposed by Zheng and Jiang [2]. Nanoelectromechanical devices based on CNTs have been considered for various applications such as precision engineering, electronic devices, medicines, etc. Gigahertz nanotube oscillators may be applied to nanoscale sensors, actuators, resonators, injectors, motors, engines, filters, memory and switching devices. Molecular dynamics (MD) has often been used to study and predict the performance of nanoscale machine components, and has been utilised to investigate multi-walled CNT oscillators [3–22]. The oscillatory behaviour of multi-walled CNT oscillators can be initialised by precision mechanical controllers [23,24], and remotely initialised with electromagnetic fields [8,9], lasers [17] and electrostatic forces [25].

CNTs encapsulating metal nanowires or clusters (M@CNTs) have been synthesised and investigated [26], and these can also be applied to a gigahertz CNT oscillator. Therefore, in this paper, an M@CNT oscillator is investigated using classical MD simulations. The oscillatory behaviours of double-walled CNT oscillators encapsulating a copper nanowire are considered. The mass-dependent frequency change cannot be estimated using classical oscillation theory when the encapsulated nanowire deforms the encapsulating CNT.

2. Methods

To perform the MD simulations for a double-walled CNT oscillator encapsulating a copper nanowire, we used two empirical potential functions. For carbon–carbon interactions, we used the Tersoff–Brenner potential function [27–29] that has been widely applied in carbon systems. The long range interactions of carbon were characterised with the Lennard-Jones 12-6 (LJ12-6) potential with the parameters obtained from Mao et al. [30]. In this work, the parameters for the LJ12-6 potential are $\varepsilon_{\text{carbon}} = 0.0042$ eV and $\sigma_{\text{carbon}} = 3.37$ Å. The cutoff distance of the LJ12-6 potential is 10 Å. In this work, since the interactions of copper–copper were not the main concern, we used a simple LJ12-6 potential function [31] with parameters $\varepsilon_{\text{copper}} = 2.277$ Å and $\sigma_{\text{copper}} = 0.415$ eV, and the cutoff distance was taken to be 2.2 s. The potential parameters were determined from the known experimental values of the cohesive energy and lattice constant at room temperature [31]. Agrawal et al. [31] showed that when using this LJ12-6 potential, the activation energies and pre-exponential factors of the self-diffusions of Cu were in good agreement with the other experimental and theoretical data. For carbon–copper, the LJ12-6 potential function with a cutoff distance of 10 Å has been used in classical MD simulations to study the carbon–copper interface [32]. The LJ12-6 potential function for carbon–copper is unsuitable for quantitative discussions on physical phenomena, because substantial charge transfer

*Corresponding author. Email: hjhwang@cau.ac.kr

ISSN 0892-7022 print/ISSN 1029-0435 online

DOI: 10.1080/08927020802301953
http://www.informaworld.com

is expected to take place between the CNT and Cu nanowires with metallic properties. However, since this work uses the LJ12-6 potential function, the Coulomb interactions between polarised electrons cannot be included and, thus, this effect should be considered in future works.

In our MD simulations, we used the same MD methods as those used in our previous studies [33–36]. The MD code uses the velocity Verlet algorithm and neighbour lists to improve the computing performance. The MD time step (Δt) was 5×10^{-4} ps. The temperatures of all the MD simulations were set to 1 K and the temperature of the outerwall was constant. The total MD times for all of the MD simulations were 1 ns.

Two double-walled CNTs of (10,10)(5,5) and (15,15)(10,10), respectively, were considered. The open outer (15,15) and (10,10) CNTs were composed of 500 and 750 atoms with a length of 3 nm and the capped inner (5,5) and (10,10) CNTs were composed of 270 and 640 atoms with a length of 3.3 nm, respectively. Figure 1 shows the atomic structure of the double-walled CNTs encapsulating the copper nanowires. The copper nanowires (of the Cu@(10,10)(5,5) and Cu@(15,15)(10,10) CNTs) consisted of 46 and 330 atoms obtained from our previous work investigating optimised copper nanowires encapsulated in armchair CNTs, respectively [37]. The initial structures were relaxed by simulated annealing simulations; then, the Cu@(10,10)(5,5) CNT was optimised without deforming, whereas the Cu@(15,15)(10,10) CNT was optimised with surface deformation because the Cu nanowire structure did not have a perfectly cylindrical shape.

CNT oscillators can be realised when the outer CNT is fixed or in contact with other materials to obtain oscillatory behaviours. Therefore, the centre-of-mass of the outer CNT of all the MD simulations was constantly maintained using the position rescaling method every MD steps. The core CNTs were initially displaced from the relaxed structures and, then, the oscillation frequencies (f) were analysed by a fast Fourier transform using the data obtained from the 300-ps MD simulations.

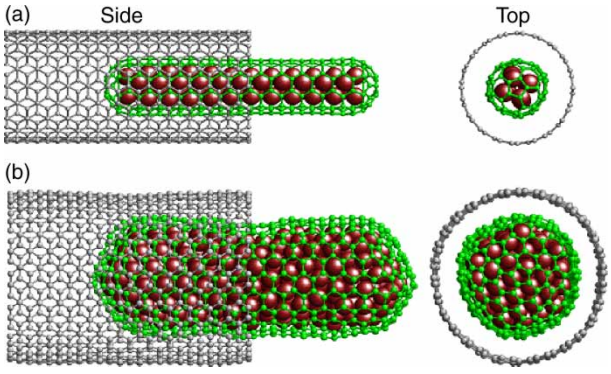

Figure 1. Atomic structure of the double-walled CNTs encapsulating copper nanowires. (a) Cu_{46}@(10,10)(5,5) CNT and (b) Cu_{330}@(15,15)(10,10) CNT oscillators. The open outer (15,15) and (10,10) CNTs were composed of 500 and 750 atoms with a length of 3 nm and the capped inner (5,5) and (10,10) CNTs were composed of 270 and 640 atoms with a length of 3.3 nm, respectively.

3. Results and discussion

The MD simulation results of the double-walled CNT oscillators were compared to those of the double-walled CNT oscillators encapsulating Cu nanowires (Cu@CNT) with various initial displacements. Figures 2 and 3 show the MD results for the Cu@(10,10)(5,5) CNT with an initial displacement of 13 Å and for the Cu@(15,15)(10,10) CNT with an initial displacement 10 Å, respectively. Figure 2(a)–(d) shows the displacements of the (5,5) CNT centre-of-mass, the total excess force (F_x) induced on the inner (5,5) CNT or Cu@(5,5) CNT, the binding energy (U_{C-Cu}) between the Cu nanowire and (5,5)(10,10) CNT, and the total inter-wall vdW energies (U_{vdW}) as functions of the MD time, respectively. Figure 3(a)–(d) shows the displacements of the (10,10) CNT centre-of-mass, the total excess force (F_x) induced on the outer (10,10) CNT or Cu@(10,10) CNT, the binding energy (U_{C-Cu}) between the Cu nanowire

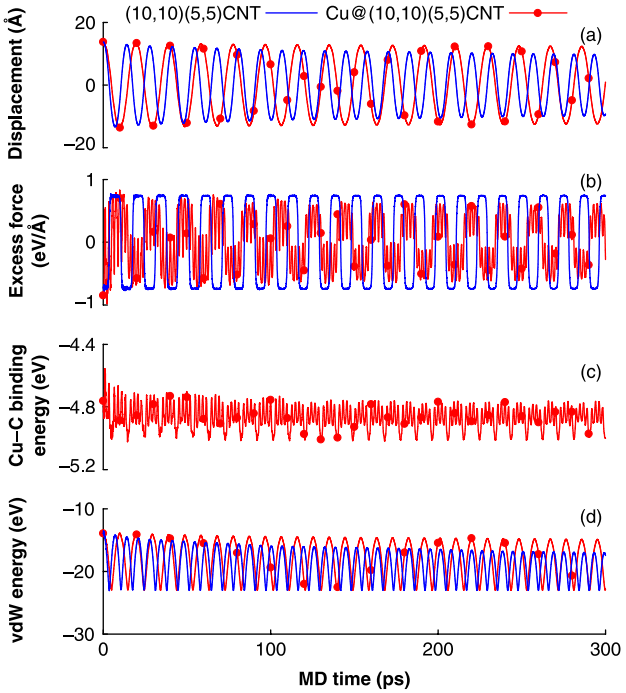

Figure 2. MD results for the Cu@(10,10)(5,5) CNT with an initial displacement of 13 Å. (a) Displacements of the (5,5) CNT centre-of-mass, (b) total excess force (F_x) for the (5,5) CNT and Cu@(5,5) CNT, (c) Cu–C binding energy (U_{C-Cu}) and (d) C–C vdW energies (U_{vdW}) as functions of the MD time.

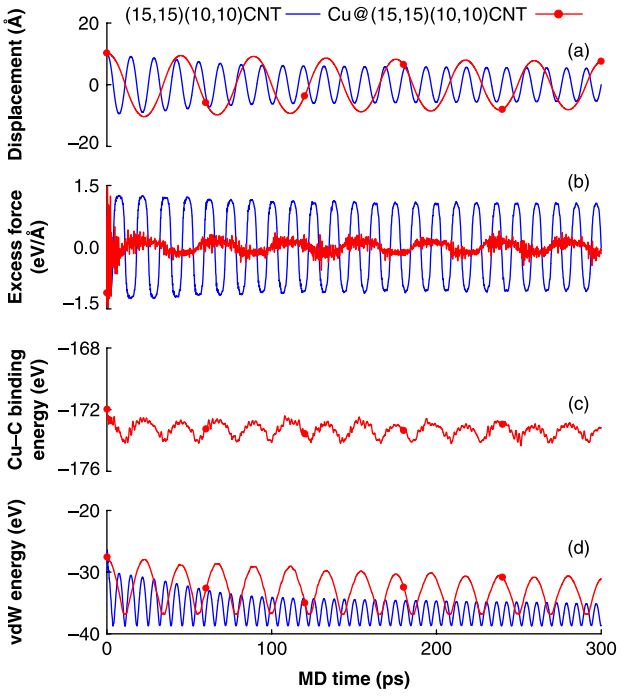

Figure 3. MD results for the Cu@(15,15)(10,10) CNT with an initial displacement of 10 Å. (a) Displacements of the (10,10) CNT centre-of-mass, (b) total excess force (F_x) for the (10,10) CNT and Cu@(10,10) CNT, (c) Cu–C binding energy (U_{C-Cu}) and (d) the C–C vdW energies (U_{vdW}) as functions of the MD time.

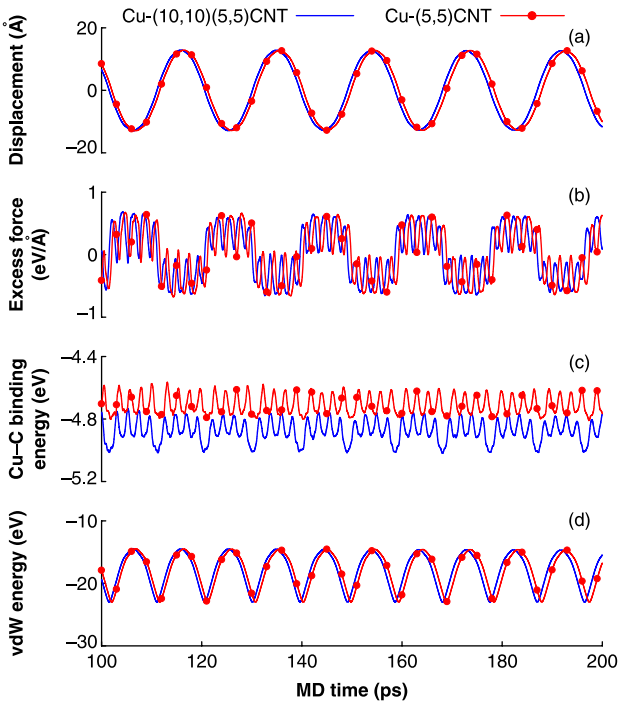

Figure 4. The MD simulation results when the copper atoms interacted with the (5,5) CNT were compared to those when the copper atoms interacted with both the (5,5) and the (10,10) CNTs. (a) Displacements of the inner CNT centre-of-mass, (b) excess forces, (c) Cu–C binding energy and (d) C–C vdW energies as functions of the MD time for the different copper–carbon interaction ranges from the 100th and 200th ps.

and (10,10)(15,15) CNT, and the total inter-wall vdW energies (U_{vdW}) as functions of the MD time, respectively. In the static calculation, the excess forces of the Cu@CNT oscillator were slightly higher than those of the CNT oscillator. The F_x of the CNT oscillators is composed of only the excess C–C vdW forces (F_{vdW}), whereas the F_x of the Cu@CNT oscillators is composed of the metal–carbon interaction force (F_{C-Cu}) as well as the F_{vdW}. For the Cu@(10,10)(5,5), the U_{C-Cu} and F_{C-Cu} were around 1% of the U_{vdW} and F_{vdW}, respectively, and for the Cu(15,15)(10,10), the U_{C-Cu} and F_{C-Cu} were around 3% of the U_{vdW} and F_{vdW}, respectively. From our calculations, the excess vdW force induced by the inter-wall interactions is 17 times higher than the excess force induced by the Cu nanowire–CNT interactions. This implies that the F_{C-Cu} effects are much lower than the F_{vdW} effect for the Cu@CNT oscillator. If the F_{C-Cu} is assumed to be zero, since the mass of the Cu@(10,10)(5,5) CNT oscillator is 1.895 times higher than that of the (10,10)(5,5) CNT oscillator, then the operation frequency (f) of the Cu@(10,10)(5,5) CNT oscillator is 0.726 times lower than that of the (10,10)(5,5) CNT oscillator in the classical oscillation theory as expressed by $2\pi f = \sqrt{k/m}$, where m is the mass of the oscillator. If we assume that the CNT oscillator approximates a classical oscillator with a spring constant, the relation between the F_x and the operating frequency ($f_{M@CNT}$) of the M@CNT oscillator could be expressed as

$$f_{M@CNT} \propto \sqrt{\frac{F_x}{m}}. \quad (1)$$

Figures 3(b) and 4(b) show that the excess forces of the Cu@CNT oscillators are less than those of the CNT oscillators. From the static calculations, the F_x of the Cu@CNT oscillator was slightly higher than that of the CNT oscillator. This difference is due to both the excess force and the mass differences of the copper and carbon atoms. Since the excess vdW force per carbon atom is 17 times higher than the excess Cu–C force per copper atom and the masses of copper atoms are 5.25 higher than those of carbon atoms, the inner CNTs are much easier to accelerate than the copper nanowires. However, since the Cu nanowires are encapsulated inside the inner CNTs, the inner CNT motions are closely related to the Cu nanowire motions. The inner CNT weakly collided with the encapsulated copper nanowire, and this repulsive force results in a decrease of the total excess force. These collisions are found in the ripples in Figures 2(b),(c) and 3(b),(c). Therefore, the low velocity of the CNT oscillator is related to its low frequency.

For the Cu@(10,10)(5,5) CNT oscillator, the interaction effect between the Cu nanowire and the outer (10,10) CNT was investigated. The MD simulation results when the copper atoms interacted with the (5,5) CNT were compared to those when the copper atoms interacted with both the (5,5) and the (10,10) CNTs. Figure 4(a)–(d) shows the displacements of the inner CNT centre-of-mass, the excess forces, the Cu–C binding energy and the C–C vdW energies as functions of the MD time for the different copper–carbon interaction ranges from the 100th to 200th ps, respectively. Figure 4 shows that the frequency in the case of the copper–(10,10)(5,5) CNT interaction is slightly higher than that in the case of the copper–(5,5) CNT interaction, and this implies that very low excess forces are achieved in the case of the interactions between the copper nanowire and the outer CNT. However, this very low excess force affected the oscillatory behaviours of the Cu@CNT, as shown in Figure 4. Our MD simulation results show that the mass-dependent frequency change is a more important factor than the copper–carbon interaction-dependent frequency change [38].

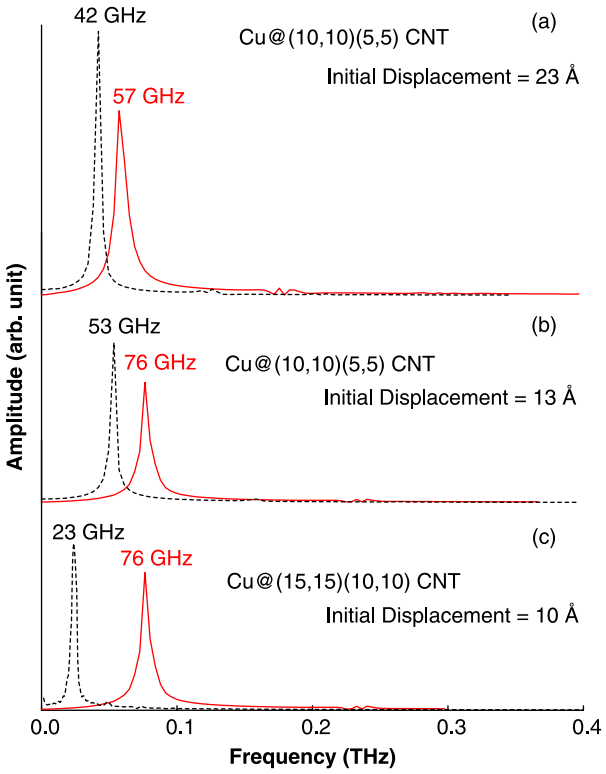

Figure 5. Frequencies of the (10,10)(5,5) CNT and the Cu@(10,10)(5,5) CNT for the initial displacements of (a) 13 and (b) 23 Å, and (c) frequencies of both the (15,15)(10,10) CNT and the Cu@(15,15)(10,10) CNT oscillators for an initial displacement of 10 Å. The solid and the dashed lines indicate the frequency spectrums for the CNT and the Cu@CNT oscillators, respectively.

Figure 5(a),(b) shows the frequencies of both the (10,10)(5,5) CNT and the Cu@(10,10)(5,5) CNT oscillators for various initial displacements. The solid and the dashed lines indicate the frequency spectrums for the (10,10)(5,5) CNT and the Cu@(10,10)(5,5) CNT oscillators, respectively. As the initial displacements were increased, the frequencies decreased. The frequencies of the CNT oscillators were 76 and 57 GHz for the initial displacements of 13 and 23 Å, respectively. This result is in good agreement with the previous works [2,3,19] that showed that the operation frequency of the CNT oscillator was inversely proportional to the square root of its initial displacement, which was predicted by an explicit formula [2,3] and was verified by Rivera et al. [19]. The frequencies of the Cu@(10,10)(5,5) CNT oscillator were 53 and 42 GHz for the initial displacements of 13 and 23 Å, respectively. For a simple linear spring-mass system, the frequency is proportional to the square root of the ratio of the spring constant to the mass, according to the classical theory. Using Equation (1) and the frequencies of the (10,10)(5,5) CNT oscillators, the corresponding frequencies of the Cu@(10,10)(5,5) CNT oscillators are found to be 55 and 41 GHz for the initial displacements of 13 and 23 Å, respectively. The systems of these oscillators are, of course, highly nonlinear, as discussed above, but nevertheless the classical theory provides a fairly good estimate.

Figure 5(c) shows the frequencies of both the (15,15)(10,10) CNT and the Cu@(15,15)(10,10) CNT oscillators for an initial displacement of 10 Å. The solid and dashed lines indicate the frequency spectrums for the (15,15)(10,10) CNT and the Cu@(15,15)(10,10) oscillators, respectively. The frequencies of the (15,15)(10,10) CNT and Cu@(15,15)(10,10) CNT oscillators were 76 and 23 GHz, respectively. For the same initial displacement, as the diameter of the double-walled CNT oscillator increases, its operating frequency decreases, as expressed by $95\exp(-2.3d)+f_{\infty}$, where d is the diameter of the outer CNT on the nanometer scale and $f_{\infty}=11.8$ GHz is the frequency of the double-walled CNT oscillator with a very large diameter [39]. For the (15,15)(10,10) CNT oscillator with an initial displacement of 10 Å, this relation provides a good estimate of 77 GHz. For the Cu@(15,15)(10,10) CNT oscillator, the frequency, 39 GHz, estimated from Equation (1), is very different from the frequency, 23 GHz, obtained from the MD simulation. While the frequencies of the Cu@(10,10)(5,5) CNT oscillator were estimated fairly and accurately by Equation (1) showing the mass–frequency dependence, the frequency of the Cu@(15,15)(10,10) CNT oscillator was not. These results, at least, can be explained by two factors. The first is the mass dependence of the encapsulated Cu nanowire. For the Cu@(10,10)(5,5) CNT oscillator, the mass of the Cu nanowire is less than that of the (5,5) CNT, whereas for the Cu@(15,15)(10,10) CNT, the mass of the Cu nanowire is 2.7 times higher than

that of the (10,10) CNT. As the proportion of the Cu nanowire's mass increases, the motion of the Cu@CNT oscillator is increasingly influenced by the Cu nanowire's mass, rather than by the CNT's mass. The ripples shown in Figures 2(b),(c) and 3(b),(c) imply the velocity decrease of the Cu@CNT oscillator. When the Cu@CNT oscillator is moving, the Cu nanowire slightly collides with the encapsulating CNT, as discussed above; then, the motion of the Cu nanowire with a large mass is more important than that of the CNT with a small mass in terms of the momentum and energy transfers. Therefore, as the size of the nanowire increases, the motion of the nanowire becomes increasingly important. However, the frequency of the Cu@(15,15)(10,10) CNT oscillator was much less than that obtained from Equation (1) showing the mass–frequency dependence. Therefore, the frequency of the Cu@(15,15)(10,10) CNT oscillator was also influenced by effects other than the mass increase effect. The second is the inter-wall friction dependence. As shown in Figure 1(a), for the Cu@(10,10)(5,5) CNT oscillator, the (5,5) CNT was not deformed and it oscillated with a very low surface friction and energy dissipation. However, for the Cu@(15,15)(10,10) CNT oscillator, the (10,10) CNT was deformed, as shown in Figure 1(b). Therefore, the deformed Cu@(10,10) CNT oscillated with a high surface friction during its translational motion, and this induced a high energy dissipation. The high surface friction led to the rotational motions of the Cu@(10,10) CNT. To visualise the rotational motion of the Cu@(10,10) CNT oscillator, the position variation of an carbon atom of the (10,10) CNT is plotted in Figure 6. Figure 6 shows the rotational motion of the (10,10) CNT for the Cu@(15,15)(10,10) CNT oscillator as a function of the MD time. The projective x_i–y_i plot exactly shows a circle due to the rotational motion of the (10,10) CNT. Figure 7(a),(b) shows the angle variations as a function of the MD time and the projective x_i–y_i plots, respectively, for both the (15,15)(10,10) CNT and the Cu@(15,15)(10,10) CNT oscillators. The rotation of the (15,15)(10,10) CNT oscillator shows an oscillation within a small angle and a periodic feature; i.e. the (10,10) CNT kept its balance in a hexagonal ring along the tangential direction of the outer tube. Therefore, the x_i–y_i plot of the (15,15)(10,10) CNT oscillator, in Figure 7(b), shows that the rotational motion of the (10,10) CNT is confined within the length of the circumference corresponding to the hexagonal ring of the CNT; i.e. this implies that the energy dissipation due to the rotational motion of the (10,10) CNT oscillator is very low. However, for the Cu@(15,15)(10,10) CNT oscillator, the periodic variation of its rotational motion could not be found, because the (10,10) CNT was deformed by the encapsulated Cu nanowire, and this can be found in the irregular rotational motions in Figures 6 and 7(a). Since the MD simulations in this work did not include the thermal effects, we could not provide information on the frequency variations and the noise effects due to the thermal motions of the double-walled CNT oscillator encapsulating the copper nanowire. Therefore, since thermal energy dissipations, inter-wall energy exchanges

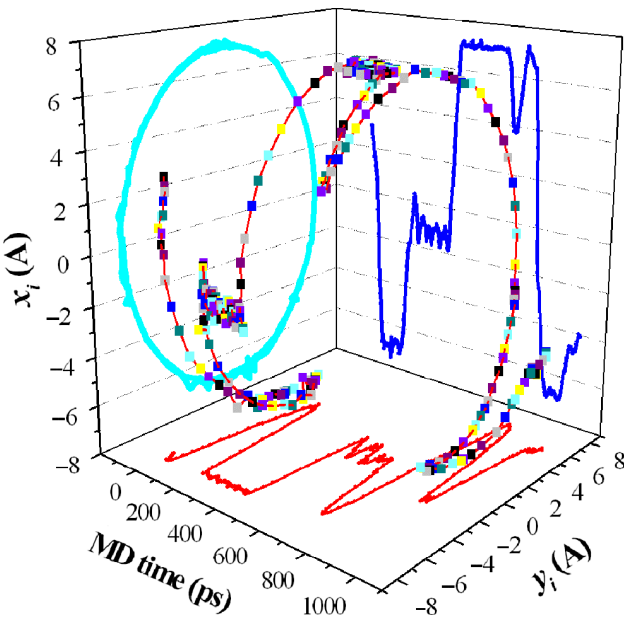

Figure 6. To visualise the rotational motion of the Cu@(10,10) CNT oscillator, the position variation of a carbon atom of the (10,10) CNT was plotted as a function of the MD time.

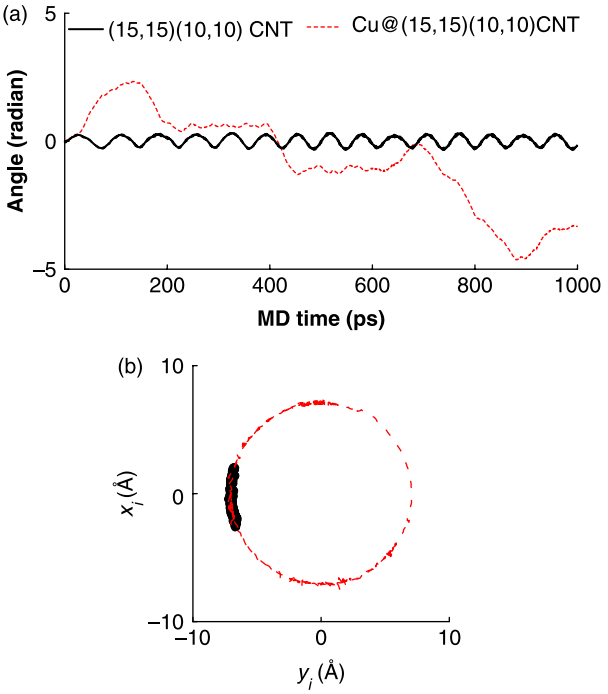

Figure 7. (a) Angle variations as a function of the MD time and (b) the projective x_i–y_i plots for both the (15,15)(10,10) CNT and the Cu@(15,15)(10,10) CNT oscillators.

and inter-wall frictions can affect the operational frequencies and oscillation damping of the multi-walled CNT oscillators, further work should be performed using MD simulations under different temperature conditions. A multi-walled CNT encapsulating a magnetic material has the potential to act as a CNT oscillator initiated by external magnetic fields, and can be used as a nano-magnetic source or nano-magnetic memory. Therefore, further investigations should be made of multi-walled CNT oscillators encapsulating magnetic nanowires. The Coulomb interactions induced by the charge transfer between the CNT and Cu nanowire should also be investigated further.

4. Summary

Double-walled CNT oscillators encapsulating a Cu nanowire were investigated by MD simulations. The excess forces of the Cu@CNT oscillator are slightly higher than those of the CNT oscillator and the excess vdW forces induced by the inter-wall interactions are 17 times higher than the excess forces induced by the Cu nanowire–CNT interactions. Since the masses of copper atoms are higher than those of carbon atoms, the latter were easier to accelerate than the former, and this induced collisions between the inner CNT and the encapsulated copper nanowire, and the consequent repulsive force decreased the total excess force. The systems of the CNT oscillators were highly nonlinear but, nevertheless, the classical oscillation theory provided a fairly good estimate of the mass dependence of the operating frequency when the CNT surface was not deformed by the Cu nanowire. However, when the encapsulating CNT was deformed by the encapsulated Cu nanowire, the frequency could not be estimated by the mass–frequency dependence.

References

[1] J. Cumings and A. Zettl, *Low-friction nanoscale linear bearing realized from multiwall carbon nanotubes*, Science 289 (2000), pp. 602–604.

[2] Q. Zheng and Q. Jiang, *Multiwalled carbon nanotubes as gigahertz oscillators*, Phys. Rev. Lett. 88 (2002), p. 045503.

[3] Q. Zheng, J.S. Liu, and Q. Jiang, *Excess van der Waals interaction energy of a multiwalled carbon nanotube with an extruded core and the induced core oscillation*, Phys. Rev. B 65 (2002), p. 245409.

[4] W. Guo, Y. Guo, H. Gao, Q. Zheng, and W. Zheng, *Energy dissipation in gigahertz oscillators from multiwalled carbon nanotubes*, Phys. Rev. Lett. 91 (2003), p. 125001.

[5] Y. Zhao, C.-C. Ma, G. Chen, and Q. Jiang, *Energy dissipation mechanisms in carbon nanotube oscillators*, Phys. Rev. Lett. 91 (2003), p. 175504.

[6] C.-C. Ma, Y. Zhao, C.-Y. Yam, G.H. Chen, and Q. Jiang, *A tribological study of double-walled and triple-walled carbon nanotube oscillators*, Nanotechnology 16 (2005), pp. 1253–1264.

[7] P. Tangney, S.G. Louie, and M.L. Cohen, *Dynamic sliding friction between concentric carbon nanotubes*, Phys. Rev. Lett. 93 (2004), p. 065503.

[8] S.B. Legoas, V.R. Coluci, S.F. Braga, P.Z. Coura, S.O. Dantas, and D.S. Galvão, *Molecular-dynamics simulations of carbon nanotubes as gigahertz oscillators*, Phys. Rev. Lett. 90 (2003), p. 055504.

[9] J.W. Kang, H.J. Hwang, and Q. Jiang, *A molecular dynamics study on oscillation of a carbon nanotube inside an encapsulating boron-nitride nanotube*, J. Comput. Theor. Nanosci. 3 (2006), pp. 880–884.

[10] J.L. Rivera, C. McCabe, and P.T. Cummings, *The oscillatory damped behavior of incommensurate double-walled carbon nanotubes*, Nanotechnology 16 (2005), pp. 186–198.

[11] P. Liu, Y.W. Zhang, and C. Lu, *Oscillatory behavior of gigahertz oscillators based on multiwalled carbon nanotubes*, J. Appl. Phys. 98 (2005), p. 014301.

[12] V.R. Coluci, S.B. Legoas, M.A.M. de Aguiar, and D.S. Galvão, *Chaotic signature in the motion of coupled carbon nanotube oscillators*, Nanotechnology 16 (2005), pp. 583–589.

[13] P. Liu, Y.W. Zhang, and C. Lu, *Analysis of the oscillatory behavior of double-walled carbon nanotube-based oscillators*, Carbon 44 (2006), pp. 27–36.

[14] J.W. Kang, O.K. Kwon, J.H. Lee, Q. Jiang, and H.J. Hwang, *Molecular dynamics study of carbon nanotube oscillator on gold surface*, Mol. Simul. 32 (2006), pp. 363–368.

[15] Y. Kimoto, H. Mori, T. Mikami, S. Kata, Y. Nakayama, K. Higashi, and Y. Hirai, *Molecular dynamics study of double-walled carbon nanotubes for nano-mechanical manipulation*, Jpn. J. Appl. Phys. 44 (2005), pp. 1641–1647.

[16] W. Guo, W. Zhong, Y. Dai, and S. Li, *Coupled defect-size effects on interlayer friction in multiwalled carbon nanotubes*, Phys. Rev. B 72 (2005), p. 075409.

[17] J.W. Kang, K.O. Song, O.K. Kwon, and H.J. Hwang, *Carbon nanotube oscillator operated by thermal expansion of encapsulated gases*, Nanotechnology 16 (2005), pp. 2670–2676.

[18] S. Xiao, D.R. Andersen, R.P. Han, and W. Hou, *Studies of carbon nanotube-based oscillators using molecular dynamics*, J. Comput. Theor. Nanosci. 3 (2006), pp. 142–147.

[19] J.J. Rivera, C. McCabe, and P.T. Cummings, *Double walled carbon nanotubes under extension: A simple nanoscale damped oscillator*, Nano Lett. 3 (2003), pp. 1001–1005.

[20] X. Zhao and P.T. Cummings, *Molecular dynamics study of carbon nanotube oscillators revisited*, J. Chem. Phys. 124 (2006), p. 134705.

[21] L.-H. Wong, Y. Zhao, G. Chen, and A.T. Chwang, *Grooving the carbon nanotube oscillators*, Appl. Phys. Lett. 88 (2006), p. 183107.

[22] Y. Zhao, C.-C. Ma, L.-H. Wong, G. Chen, Z. Xu, Q. Zheng, Q. Jiang, and A.T. Chwang, *Quasi-reversible energy flows in carbon-nanotube-based oscillators*, J. Comput. Theor. Nanosci. 3 (2006), pp. 852–856.

[23] J. Cumings and Z. Zettl, *Localization and nonlinear resistance in telescopically extended nanotubes*, Phys. Rev. Lett. 93 (2004), p. 086801.

[24] S. Akita and Y. Nakayama, *Interlayer sliding force of individual multiwall carbon nanotubes*, Jpn. J. Appl. Phys. 42 (2003), pp. 4830–4833.

[25] J.W. Kang, K.O. Song, H.J. Hwang, and Q. Jiang, *Nanotube oscillator based on a short single-walled carbon nanotube bundle*, Nanotechnology 17 (2006), pp. 2250–2258.

[26] M. Monthioux, *Filling single-wall carbon nanotubes*, Carbon 40 (2002), pp. 1809–1823.

[27] J. Tersoff, *Empirical interatomic potential for silicon with improved elastic properties*, Phys. Rev. B 38 (1988), pp. 9902–9905.

[28] ———, *Modeling solid-state chemistry: Interatomic potentials for multicomponent systems*, Phys. Rev. B 39 (1989), pp. 5566–5568.

[29] D.W. Brenner, *Empirical potential for hydrocarbons for use in simulating the chemical vapor deposition of diamond films*, Phys. Rev. B 42 (1990), pp. 9458–9471.

[30] Z. Mao, A. Garg, and S.B. Sinnott, *Molecular dynamics simulations of the filling and decorating of carbon nanotubules*, Nanotechnology 10 (1999), pp. 273–277.

[31] P.M. Agrawal, B.M. Rice, and D.L. Thompson, *Predicting trends in rate parameters for self-diffusion on FCC metal surfaces*, Surf. Sci. 515 (2002), pp. 21–35.

[32] S. Dorfman, K.C. Mundim, D. Fuks, A. Berner, D.E. Ellis, and J. Van Humbeeck, *Atomistic study of interaction zone at copper–carbon interfaces*, Mater. Sci. Eng. C 15 (2001), p. 191.

[33] J.W. Kang, S.C. Kong, and H.J. Hwang, *Electromechanical analysis of suspended carbon nanotubes for memory applications*, Nanotechnology 17 (2006), pp. 2127–2134.

[34] J.W. Kang and H.J. Hwang, *Operating frequency in a triple-walled carbon-nanotube oscillator*, J. Korean Phys. Soc. 49 (2006), pp. 1488–1492.
[35] J.W. Kang and Q. Jiang, *Electrostatically telescoping nanotube nonvolatile memory device*, Nanotechnology 18 (2007), p. 095705.
[36] J.W. Kang, O.K. Kwon, and J.H. Lee, *Multi-walled carbon nanotube oscillators as multi-frequency generators for nano embedded systems*, J. Comput. Theor. Nanosci. 5 (2008), pp. 290–293.
[37] W.Y. Choi, J.W. Kang, and H.J. Hwang, *Structures of ultrathin copper nanowires encapsulated in carbon nanotubes*, Phys. Rev. B 68 (2003), p. 193405.
[38] J.W. Kang, Q. Jiang, and H.J. Hwang, *A double-walled carbon nanotube oscillator encapsulating a copper nanowire*, Nanotechnology 7 (2006), pp. 5485–5490.
[39] J.W. Kang and J.H. Lee, *Frequency characteristics of triple-walled carbon nanotube gigahertz devices*, Nanotechnology 19 (2008), p. 285704.